ISSN 1333-1124

TRANSACTIONS

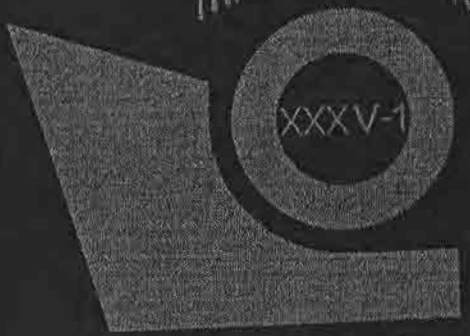

of FAMENA

Zagreb
2011

Transactions of FAMENA

UNIVERSITY OF ZAGREB

FACULTY OF MECHANICAL ENGINEERING AND NAVAL ARCHITECTURE

✉ *HR – 10 000 ZAGREB, Ivana Lučića 5*

☎ *01 61 68 540 / Fax 61 68 187*

e-mail: jasna.biondic@fsb.hr

http://famena.fsb.hr/famena.php

Printed by:

Stega tisak d.o.o., Zagreb

TRANSACTIONS

of FAMENA

Contents

VOLUME 35, No. 1 Zagreb 2011

[7] Reibenschuh, M., Cus F., Zuperl U.: Machining of hard steel alloys with new prototypes of cutting tools, Proceedings of the 21st International DAAAM Symposium, Zadar, 2010, pp 1157-1158.

[8] Park S. H.: Robust Design and Analysis for Quality Engineering, Chapman and Hall, London 1996

[9] Hu, Y. H., Hwang, J. N.: Handbook of neural network signal Processing, Electrical Engineering & Applied Signal Processing Series 5, CRC Press, 2001.

[10] Bishop, C. M.: Neural networks for pattern recognition, Oxford Univ. Press Cambridge, 1995

Submitted: 15.11.2010

Accepted: 04.3.2011

Nikola Gjeldum
Ivica Veža
Boženko Bilić
University of Split, Faculty of Electrical Engineering, Mechanical Engineering and Naval Architecture
R. Boškovića 32, 21000 Split, CROATIA
E-mail: nikola.gjeldum@fesb.hr

Miroslav Mijajlović
Dragan Milčić
Dušan Stamenković
Aleksandar Živković

ISSN 1333-1124

MATHEMATICAL MODEL FOR GENERATED HEAT ESTIMATION DURING THE PLUNGING PHASE OF FSW PROCESS

UDC 621.791.1

Summary

The friction stir welding (FSW) process starts when the welding tool rotates and plunges into the base material. Significant amount of mechanical energy given to the welding tool is used to overcome resistances in the base material and as a result, this mechanical energy transforms into heat. Experimental studies have shown that extreme values of the resistance forces and maximum engagement of the welding machine power appear during plunging. This leads to the conclusion that the FSW process has to fulfil welding requirements as well as to overcome resistances. Since it is expected that maximal power consumption during FSW appears when the maximum value of heat is generated, the FSW process has to be designed according to this power consumption. An adequate and precise mathematical model for generated heat estimation can be used for the FSW process design The verification of the mathematical model validity can be done by comparison of the analytical with the experimental values of consumed power.

Key words: *friction stir welding, heat generation*

1. Introduction

Friction stir welding (FSW) is a solid state welding process predominantly used for joining materials difficult to weld by applying some of conventional processes. Its application is mainly connected with the welding of aluminium, aluminium alloys and other soft metals/alloys [1]. In comparison to other welding processes, FSW delivers the smallest amount of energy to the base metal, which results in the smallest deformation in the structure of the base metal. However, FSW is still an unconventional welding process because of the complexity of application and the need for long welds in order to have great productivity. FSW is used for plate-shaped parts.

In FSW, a cylindrical, shouldered tool (Figure 1) with a profiled threaded/unthreaded probe is rotated at a constant speed and fed at a constant traverse speed into the joint line between two plates (base material), which are butted together. The parts are clamped rigidly onto a backing plate in a manner that prevents the abutting joint faces from being forced apart. The length of the probe is slightly smaller than the required weld depth with the goal of

enabling contact between the tool shoulder and the base material when maximal plunging is achieved. The probe is moved against the weld-joint line or vice versa.

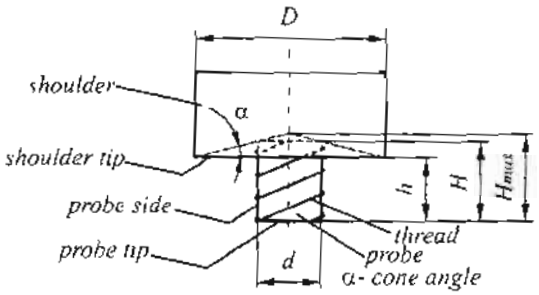

Fig. 1 Welding tool

FSW was patented in 1991 [1] and in 1992, the industrial application of the process started. At the beginning, the application of FSW based on experimental studies only. Studies aimed at optimizing technological parameters of the FSW process. Nowadays, numerous scientists conduct experimental studies in order to improve process parameters, by improving the welding tool, weld quality etc., however. At the same time, the development of mathematical models of FSW also took place. Previous papers on modelling the FSW process include analytical (thermal) models, finite element (FE) based solid thermal and thermo-mechanical models, fluid dynamic models, and stress and strain conditions of the base material. Some of these models include heat generation from the FSW tool and assumptions are made regarding the interface condition, which all have their drawbacks and limitations. Santiago et al. [2] introduced a model of the FSW process, using a finite element based program with a reproduction of the temperature field and volume flow in the FSW process. Numerical results were compared with experimental results and discussed. Gould et al. [3] developed an analytical heat transfer model for FSW based on the Rosenthal equation [4], quasi-stationary temperature field over a semi-infinite plate with a moving heat source. Chen and Kovačević [5, 6] carried out thermal and thermo-mechanical analyses using finite elements. These analyses are based on a heat source model, without considering the thermo-mechanical coupling generated by the plastic flow. Song and Kovacevic [6] investigated the influence of the preheating (dwell) period on the temperature fields. They assume the existence of sliding condition between welding tool and base material and use an effective friction coefficient and experimental plunge force in the heat source expression. Ulysse [7] presented 3D modelling of FSW using fully coupled thermo-mechanical viscoplastic flow models with good results where plastic deformations commonly occur. Due to geometric and kinematic characteristics of FSW, the problem is mainly 3D. This kind of modelling was done by Colegrove et al. [8] by using the "CFD package FLUENT", where a coupled thermo-mechanical viscoplastic model for aluminium material was solved and promising results were obtained as regards the material flow distribution. Nandan et al. [9, 10] reported results of a stainless steel FSW simulation by using this kind of models with good agreement between the computed temperature field and the experimental data, showing the versatility of the viscoplastic flow models to represent large deformation processes in FSW. In the model by Chao et al. [11], heat generation comes from the assumption about the existence of sliding friction, where Coulomb's law is used to estimate shear or friction force at the interface. The pressure at the welding tool-base material contact is assumed to be constant, thereby enabling the radially dependent surface heat flux distribution as a representation of the friction heat generated by the tool shoulder, but neglecting heat generated by the probe surfaces. Frigaard et al. [12, 13] modelled the heat input from the tool shoulder and the probe as fluxes on

squared surfaces at the top and sectional planes on a 3D model and control the maximum allowed temperature by the adjustment of the friction coefficient at elevated temperatures. Russell et al. [14] based heat generation on a constant friction stress at the interface, equal to the shear yield stress at an adequate temperature, which is set to app. 5% of the yield stress at room temperature. The heat input is applied as a point source or line source as in the normal version of Rosenthal's equations, but the solution is modified to account for the limited extent of the plate width. Colegrove [15] used an advanced analytical estimation of heat generation for tools with a threaded probe to estimate the heat generation distribution. The fraction of heat generated by the probe is estimated to be as high as 20%, which leads to the conclusion that the analytical estimated probe heat generation contribution is not negligible. Along with the mathematical stress model, Colegrove [15] developed a material flow model, which addressed the influence of threads on the material flow. An advanced viscous material model was introduced and the influence of different contact conditions prescribed as the boundary condition was analysed. A thorough presentation of analytical estimates of heat generation in FSW is also included in [16]. Xu et al. [17] introduced a 2D solid mechanical FE model using ABAQUS Explicit and a 2D CFD model using Fluent, and the main objective was to reveal the material flow around the probe. The FE model included two different submodels with different contact conditions at the probe/material interface: the sliding interface and the frictional contact model. The material surrounding the probe was exposed to a temperature field obtained from the experiment, with the calculation of yield stress for the thermal material response. The flow results were qualitatively compared with the experimental flow visualization via the marker insert technique. Some of the limitations of the models are the missing influence of the tool shoulder and the lack of heat generation. The 2D CFD model gave similar results as the two-dimensional FE model, which used a boundary condition at the tool/metal interface. Khandkar et al. [18] introduced a torque based heat input model, where the torque/power known from experiments was used in the expression for the heat source. Inverse modelling for the estimation of the friction coefficient/heat source is not necessary as opposed to the models presented by [6, 11, 14, 15]. This enables an investigation into other important parameters, e.g. different heat transfer coefficients at the bottom of the base material, base material/backing plate gap conductance and backing plate conductivity. Similarly, Shi et al. [19] used the experimentally observed mechanical power as input in a thermo-mechanical 3D FE model. The model investigated the influence of tool loads (torque and plunge force) on residual stresses.

Having recognized generated heat as one of the most important parameters of FSW, numerous scientists have been working on an adequate mathematical model capable of describing the heat generation process within FSW more accurately. Probably, the greatest difficulty in the development of such a mathematical model is existence of numerous parameters that appear and describe the friction process (friction coefficient, contact pressure, stress, strain, temperature, etc.). Parameters are mutually connected and dependent one on another. These dependences are mostly complex and in most of the previous studies they were replaced with numerous approximations which gave some results that are limitedly usable.

This paper analyzes heat generation during the plunging phase of the FSW process without a deeper analysis of the heat generation physics, assuming conditions on the welding tool-base material contact, giving a detailed geometrical and time dependent analysis of the friction contact between the welding tool and the base material. Based on that analysis, a possible mathematical model with analytical expressions for the estimation of heat generated in the plunging phase is presented. These analytic results are compared to the results given by Schmidt et al. [20].

2. Phases of FSW

FSW consists of several active phases in which the welding tool and the base material relatively move, one to another, throughout every phase (Figure 2). During the first phase, the welding tool plunges into the base material at the starting point of the joint line. When the welding tool reaches the maximum plunging depth, the plunging phase is finished and the dwelling phase starts. During the dwelling phase, the welding tool, inserted into the base material, rotates but it is held steady relative to the base material. The mechanical contact between the welding tool and the base material generates heat by tribological processes. Heat dissipates into the surrounding space. This results in the softening of the base material. When the material becomes soft enough the welding phase starts – with transversal movement of the welding tool or the base material along the joint line. The welding phase lasts until the complete distance of the weld is covered. If necessary, the welding tool starts the second dwelling phase to stabilize the welding process and to finish welding. After the second dwelling, the welding tool is pulled out from the base material, the pulling out phase, and the FSW process is over.

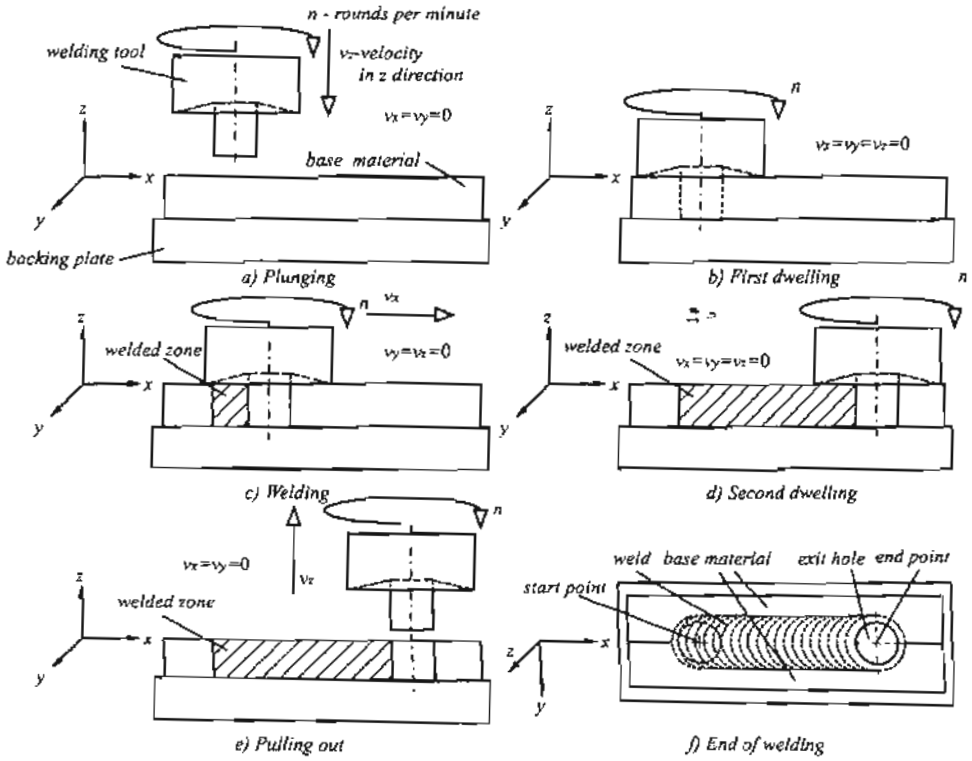

Fig. 2 Phases of FSW process

The welding phase is the only productive phase in FSW. All other phases prepare or finish the weld creation and their influence on the quality of the weld is notable.

3. Plunging phase

At the beginning, the welding tool is positioned above the starting point on a joint line and rotates (Figure 2, a). The first contact between the welding tool and the base material is achieved between the probe tip and the top surface of the base material. As a result, friction between them occurs and it opposes the rotation of the welding tool.

This frictional contact consumes some amount of mechanical energy given to the welding tool and transforms it into heat. This heat dissipates into the surrounding material and increases the temperature of the base material. The base material is loaded with the plunging force $F(t)$ and the torsion momentum of the welding tool $M(t)$. These loads stress the base material; the base material suffers contact pressure (normal stress) and shear stress (tangent stress).

Since the process of friction appears between two metallic bodies, the welding tool and the base material, Bowden and Tabor [21] suggest that the friction coefficient μ on such a contact can be given as:

$$\mu = \tau / p \tag{1}$$

where: τ – tangent shear stress of the softer material (in this case: welding pieces) and p – contact pressure (normal stress at the contact of the welding tool and the base material).

If plunging force $F(t)$, variable during time t, is deployed on the welding tool over the probe with a diameter of d, considering the rotation of the welding tool to be constant (angular rotation speed $\omega = const.$), contact pressure on radial distance r from the rotation axis is [22]:

$$p(r,t) = \frac{F(t)}{2 \cdot \pi \cdot \frac{d}{2} \cdot \sqrt{\left(\frac{d}{2}\right)^2 - r^2}}, \; 0 \le t < t_{pl}, \; 0 \le r \le \frac{d}{2} \tag{2}$$

where t_{pl} – duration of the plunging phase.

The median value of the contact pressure $p_m(t)$ on the contact is:

$$p_m(t) = \frac{4 \cdot F(t)}{d^2 \cdot \pi}, \; 0 \le t < t_{pl}. \tag{3}$$

At the beginning of the plunging phase (Fig. 3, a), the plunging force pushes the probe into the base material. The base material elastically deforms but there is no significant penetration of the welding tool; the contact pressure has not reached the values of the base material elasticity limit (considered equal to the yield strength σ_{Yield}) and the material is capable of resisting plunging without any or with minor plastic deformations. An increase in the plunging force results in an increase in the contact pressure and in some areas the contact pressure exceeds the value of the elasticity limit and the material is plastically deformed (Fig. 3, b). However, these areas are surrounded with the elastically deformed material that is resisting plunging and intensive plunging of the welding tool still does not exist. A further increase in the plunging force intensity increases the contact pressures above the value of the elasticity limit on the complete contact area. This makes the complete area under plastic deformation but the plunging depth of the welding tool still does not reach a notable value. Completely plasticized and a bit softer than at the beginning of plunging, the material still

resists the plunging because of the surrounding elastically deformed area that is capable of resisting deformation. This suggests that plunging can be achieved only when the value of contact stress becomes much higher than the elasticity limit and the area of contact and the area near the contact becomes completely plastic.

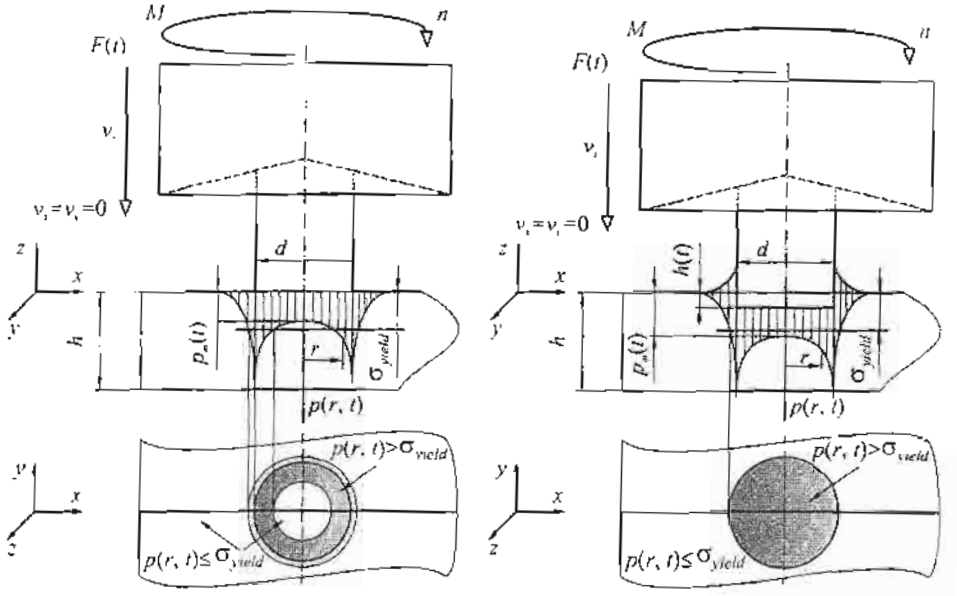

a) no plastic deformation and no notable plunging

b) some plastic deformations and some plunging

Fig. 3 The contact pressure distribution

Bowden and Tabor [21] have shown that if the median contact pressure p_m (t) has an intensity less than 1.5 · σ_{yield}, the material in contact will be stressed purely elastically (Figure 4). If the median contact pressure p_m (t) has intensity greater than 1.5 · σ_{yield}, the material enters the plastic condition but still there is sufficient elastic material to prevent the plunging of the tool. When the mean contact pressure reaches the value of p_m (t) = (2 ÷ 3) · σ_{yield} [21, 23, 26], the material becomes plastic and the welding tool plunges into the base material (Figure 4). This value of the mean contact pressure has the values of p_m (t) = (2.1 ÷ 2.3) · σ_{yield} for aluminium and aluminium alloys [21, 23].

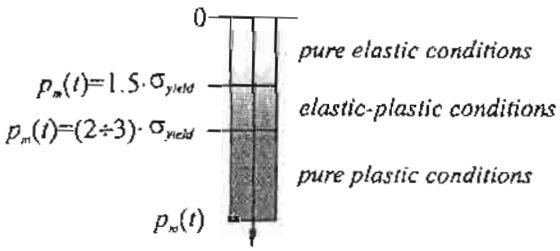

Fig. 4 Scheme of elastic and plastic conditions in material during plunging contact [25]

Yield strength (elasticity limit) is a property of material that is not dependent on loads (e.g. pressure) but it changes its value when temperature and the plastic strain rate of the material change. As mentioned earlier, the welding tool rotates while it plunges into the base material and the friction contact consumes part of mechanical energy and transforms it into heat. Heat changes the temperature of the base material and the value of the yield strength of the base material changes in the contact area, as well. For pure elastic and/or elastic-plastic conditions of the pressed material, yield strength is functionally dependent only on the temperature (T) of the material in the contact area [20]:

$$\sigma_{yield} = \sigma_{yield}(T). \tag{4}$$

The combination of pressure and rotation of the welding tool induces shear stress in the base material in a layer of material near the contact surface. Comparing the von Mises yield criterion in the uniaxial tension [25] with pure shear, the yield shear strength τ_{yield} can be estimated as:

$$\tau_{yield} = \sigma_{yield} / \sqrt{3}. \tag{5}$$

4. Heat generation

During the contact of two bodies that are pressed and relatively moving one to another, heat is generated on the contact surface or in a layer of the softer material close to the contact surface. In both cases the uniform contact shear stress $\tau_{contact}$ appears.

The welding tool has three active surfaces that are involved in heat generation: the probe tip, the probe side and the shoulder tip (Fig. 1). Total heat generated on the probe tip (pt), the probe side (ps) and the shoulder tip (st) can be estimated as [20, 27, 31]:

$$Q_{pt} = \frac{2}{3} \cdot \pi \cdot \omega \cdot \tau_{contact} \cdot \left(\frac{d}{2}\right)^3, \tag{6}$$

$$Q_{ps} = 2 \cdot \pi \cdot \omega \cdot \tau_{contact} \cdot \left(\frac{d}{2}\right)^2 \cdot h, \tag{7}$$

$$Q_{st} = \frac{2}{3} \cdot \pi \cdot \omega \cdot \tau_{contact} \left[\left(\frac{D}{2}\right)^3 - \left(\frac{d}{2}\right)^3\right] \cdot (1 + \tan\alpha) \tag{8}$$

Heat generation happens mainly during two physical processes: sticking (deformation) and sliding (adhesion) [20, 26, 27, 28]. In both cases, contact shear stress $\tau_{contact}$ is involved, but it has different physical nature for both processes.

If sticking appears, contact shear stress can be estimated as:

$$\tau_{contact} = \tau_{yield} = \sigma_{yield} / \sqrt{3}. \tag{9}$$

And if sliding appears, contact shear stress can be estimated as:

$$\tau_{contact} = \mu \cdot p_{in}(t). \tag{10}$$

5. Experiment on FSW heat generation

Schmidt et al. [20] provided some data about FSW gathered during the experiment. The welding tool used in the experiment (Figure 1) had an interchangeable threaded probe of d= 6 mm in diameter and a maximal probe length of $H_{max} \approx 6$ mm. The shoulder of diameter D = 18 mm had a cone angle of $\alpha = 10°$. Thread pitch was $P = 0.8$ mm and it was left oriented. The base material (Fig. 5) was made of aluminium alloy 2024 T3 [32], h= 3 mm thick, B/2 = 60 mm wide (each) and L = 150 mm long. The experiment was conducted on an adapted CNC milling machine with the rotation speed of n = 400 revolutions per minute (n = 41.87 rad/s), with the transversal welding speed of v_x = 2 mm/s. The weld has been created on a length of l = 105 mm, starting at the point on the joint line 15 mm away from the edge. The data acquisition system, mounted on the milling head, monitored torque M (t) on the welding tool and plunging force F (t), both along z-axis. The value of experimental power P (t) has been calculated by integrating the torque and the rotation speed.

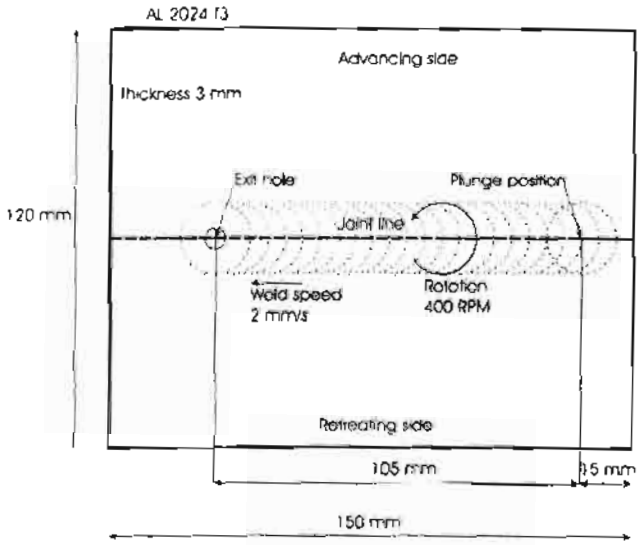

Fig. 5 Work piece geometry and welding parameters [20]

Durations of the FSW phases were [20]:

- plunging: from 0 s to 8.7 s, duration t_{pl} = 8.7 s;
- first dwelling: from 8.7 s to 13.7 s, duration: t_{d_1} = 5 s;
- welding: from 13.7 s to 66.2 s, duration: t_w = 52.5 s;
- second dwelling: from 66.2 s to 71.2 s, duration: t_{d_2} = 5 s;
- pulling out: this value has not been recorded.

The maximal temperature of the base material was monitored on the centreline on the top surface of the base material, and it was T_{max} = 400 °C during the FSW process [20].

6. Analytical estimation of generated heat during plunging phase

The total amount of generated heat Q is a sum of heat generated on all active surfaces:

$$Q = Q_{pt} + Q_{ps} + Q_{st}. \tag{11}$$

Every constituent of the total generated heat Q (from equations 6, 7 and 8) is a sum of the sliding based component Q^{sl} and the sticking based component Q^{st}:

$$Q_{pt} = (1-\delta)\cdot Q_{pt}^{sl} + \delta \cdot Q_{pt}^{st}, \tag{12}$$

$$Q_{ps} = (1-\delta)\cdot Q_{ps}^{sl} + \delta \cdot Q_{ps}^{st}, \tag{13}$$

$$Q_{st} = (1-\delta)\cdot Q_{st}^{sl} + \delta \cdot Q_{st}^{st}. \tag{14}$$

where: δ – dimensionless slip rate, contact state variable which defines the contact condition.

For $\delta = 1$ pure sticking condition is expected, while for $\delta = 0$ pure sliding condition is expected, $0 < \delta < 1$ – a combination of sticking and sliding condition is expected during the contact between the tool and the welding plate [20].

When the plunging phase starts and the welding tool touches the top surface of the base material, only the probe tip (pt) generates heat. The base material is capable of resisting plunging and there is no intensive plastic deformation. At this moment, the probe tip is only capable of sliding over the base material ($\delta = 0$). This condition will remain until the median value of the contact pressure does not reach the critical value:

$$p_m(t) \le k \cdot \sigma_{yield}, \tag{15}$$

where $k \approx 2.17$ for aluminium alloys [26].

Using equations 3 to 15, the total generated heat can be estimated as:

$$Q = Q_{pt} = Q_{pt}^{sl} = \frac{1}{3}\cdot\omega\cdot\mu\cdot F(t)\cdot d, \quad F(t) \le \frac{\pi}{4}\cdot k\ d^2\cdot\sigma_{yield}(T), \tag{16}$$

The coefficient of friction is considered to be constant and equal to $\mu = 0.3$ for all active contact surfaces as a weak approximation of a realistic friction process [28, 30].

Plunging force $F(t)$ is a characteristic of the machine and the FSW process itself and it is difficult to determine the correct intensity and behaviour analytically. In this case, for the generated heat estimation the experimental value of the plunging force, monitored during the experiment, is taken [20]. Yield strength σ_{yield} is changing as the temperature of the base material changes. Thermo-mechanical properties of the material 2024 T3 are given in the Table 1.

Table 1 Thermo-mechanical properties (no plastic strain) of material 2024 T3 [33]

T, °C	24	100	149	204	260	316	371	400
σ_{yield}, N/mm^2	345	331	310	138	62	41	28	21

When the median value of the contact pressure overcomes critical pressure $p_m(t) > k \cdot \sigma_{yield}$, the plunging of the welding tool into the base material becomes intensive. The intensive plunging forces other active surfaces (probe side, shoulder tip) to become involved in heat generation.

The probe forces into the base material, the plunging depth of the probe $h(t)$ increases (Fig. 3, b), and the probe pushes some of the softened base material upwards. The material being pushed upwards by the probe slides over the probe side and deposes under the shoulder tip. At the beginning of the intensive plunging the shoulder tip has no contact with the base material or the deposed material. An increase in the plunging depth $h(t)$ and growing volume of the deposed material eventually put the shoulder tip in contact with the base material. From that moment, the shoulder tip constantly slides over the material and partially sticks to it.

It is necessary to make some assumptions in order to estimate heat generated during the intensive plunging:

- Dimensionless slip rate for the probe tip and the shoulder tip is $\delta = 0.5$ – sticking and sliding have the same influence in heat generation on the probe / shoulder tip,
- Dimensionless slip rate for the probe side is $\delta = 0.0$ – the probe side does pure sliding,
- Shoulder tip will engage in heat generation when the plunging depth reaches the value of $h(t) \approx 0.67 \cdot h$, that is approximately $t \approx 7.6$ s after the beginning of plunging [26].

Finally, total generated heat Q equals:

$$Q = Q_{pt} + Q_{ps} + Q_{st},\ F(t) > k\ \sigma_{yield}(T) \cdot \frac{d^2 \cdot \pi}{4}, \tag{17}$$

where:

$$Q_{pt} = \frac{Q_{pt}^{st} + Q_{pt}^{sl}}{2} = \frac{1}{6} \cdot d \cdot \omega \cdot \mu \cdot F(t) + \frac{\pi \sqrt{3}}{72} \cdot d^3 \cdot \omega \cdot \sigma_{yield}, \tag{18}$$

$$Q_{ps} = Q_{ps}^{sl} = 2 \cdot \mu \cdot \omega \cdot F(t) \cdot h(t), \tag{19}$$

$$Q_{st} = \begin{cases} (1-\delta) \cdot Q_{st}^{sl} + \delta \cdot Q_{st}^{sl} = 0, & h(t) < \frac{2}{3} \cdot h \\ \frac{Q_{st}^{sl} + Q_{st}^{st}}{2} = \frac{\pi \cdot (1 + \tan\alpha)}{24} \cdot \omega \cdot \left(D^3 - d^3\right) \cdot \left[\frac{\mu \cdot 4 \cdot F(t)}{d^2 \cdot \pi} + \frac{\sigma_{yield}}{\sqrt{3}}\right], & h(t) \geq \frac{2}{3} \cdot h. \end{cases} \tag{20}$$

6.1 Temperature of base material during plunging phase

Temperature of the base material during the plunging phase can be modelled as a 3D heat transfer problem with a moveable heat source [6, 29]. The problem of the temperature field determination starts with the heat equation:

$$\rho \cdot c \cdot \frac{\partial T}{\partial t} = \lambda \cdot \left(\frac{\partial^2 T}{\partial x^2} + \frac{\partial^2 T}{\partial y^2} + \frac{\partial^2 T}{\partial z^2}\right) + q_v \tag{21}$$

where: ρ = 2700 kg/m
of aluminium; $\bar{\sigma}$ Tic
thermal conductivit
spatial derivatives
respectively; q_v, W/

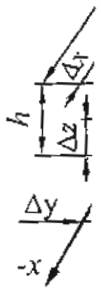

Volume hea
material V:

$$q_v = \int_V$$

The heat eq
base material vol
conditions for the
equation solving a

Initial condi
material and the s

$$T(x,$$

where T_0 = 20 °C

Boundary c
material has cons

where: $\rho = 2700$ kg/m^3 – median density of aluminium alloys: $c = 900$ J/(kg·°C) – specific heat of aluminium; $\partial T/\partial t$ – rate of temperature change at a point over time; $\lambda = 300$ W/(m·°C) – thermal conductivity coefficient for aluminium-air contact; $\partial^2 T/\partial x^2$, $\partial^2 T/\partial y^2$, $\partial^2 T/\partial z^2$, – second spatial derivatives (thermal conductions) of temperature in the x, y, and z directions, respectively; q_v, W/m^3 – volume heat density.

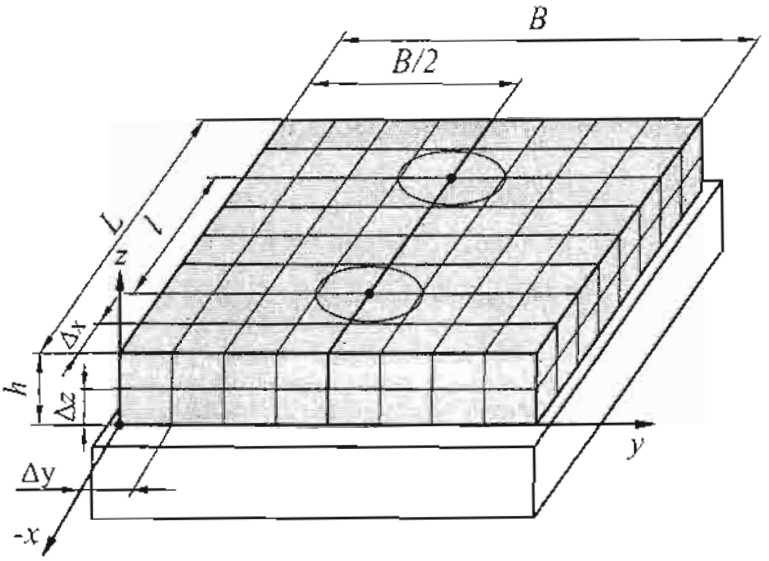

Fig. 6 Discrete model of base material (an example)

Volume heat density q_v depends on the total amount of heat Q given to the volume of material V:

$$q_v = \int_V \frac{dQ}{dV}. \tag{22}$$

The heat equation can be solved numerically, which requires the discretization of the base material volume, the discretization of time and the setting up of initial and boundary conditions for the base material. An approximation: all thermal coefficients used during heat equation solving are considered to be constant values.

Initial conditions for the base material assume temperature balance between the base material and the surrounding:

$$T(x, y, z, t)_{t=0} = T_0, \tag{23}$$

where $T_0 = 20$ °C – initial temperature of the base material and the surrounding.

Boundary conditions for the base material are different on surfaces whereas the base material has contact with atmosphere or with another solid body (Figures 7 and 8).

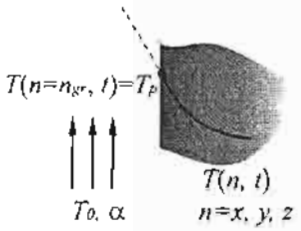

Fig. 7 Boundary conditions: metal-air contact

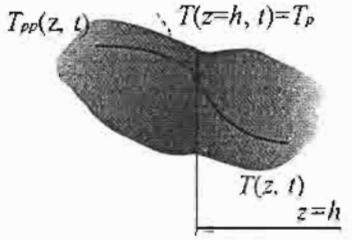

Fig. 8 Boundary conditions: metal-metal contact

Mathematical expression of the boundary conditions for metal-air contact is:

$$-\lambda\cdot\left(\frac{\partial T}{\partial x}\right)_{x=0}=\alpha\cdot\left(T_{p,x=0}-T_0\right),\quad -\lambda\cdot\left(\frac{\partial T}{\partial x}\right)_{x=L}=\alpha\cdot\left(T_{p,x=L}-T_0\right), \tag{24}$$

$$-\lambda\cdot\left(\frac{\partial T}{\partial y}\right)_{y=0}=\alpha\cdot\left(T_{p,y=0}-T_0\right),\quad -\lambda\cdot\left(\frac{\partial T}{\partial x}\right)_{y=B}=\alpha\cdot\left(T_{p,y=B}-T_0\right), \tag{25}$$

$$-\lambda\cdot\left(\frac{\partial T}{\partial z}\right)_{z=h}=\alpha\cdot\left(T_{p,z=h}-T_0\right) \tag{26}$$

where: α = 15 W/(m^2·°C) – convection heat transfer coefficient for aluminium-air contact, $T_{p,x=0}$, $T_{p,x=L}$, $T_{p,y=0}$, $T_{p,y=B}$, $T_{p,z=h}$ – temperature on the surface normal to x, y and z axis, respectively.

For z = 0, where the welding plate has contact with the working table of the milling machine, the mathematical expression of the boundary conditions for the metal-metal contact are:

$$-\lambda\left(\frac{\partial T}{\partial z}\right)_{z=h}=-\lambda_{pp}\left(\frac{\partial T_{pp}}{\partial z}\right)_{z=h} \tag{27}$$

where λ_{pp} is thermal conductivity coefficient for aluminium-steel contact and T_{pp} is temperature of the milling machine working table (steel plate).

However, this boundary condition set will make the solution of Equation 15 more complex and the approximation set that will be used is:

$$-\lambda\cdot\left(\frac{\partial T}{\partial z}\right)_{z=0}=\alpha_{sim}\cdot\left(T_{p,z=h}-T_0\right) \tag{28}$$

where α_{sim} = 3000 W/(m^2·°C) – convection heat transfer coefficient for aluminium-steel contact.

The numerical solution of heat equation for the proposed initial and boundary conditions is a set of temperatures ($T_{i,k,p,z}$) in a specific, discrete moment of time (t), for discrete points on the welding plate (coordinates: x, y, z).

6.2 Analytically versus experimentally generated heat

Figure 9 shows temperatures of some specific points on the base material. The temperatures are calculated for discrete moments of time during the plunging phase. The coordinates of the points in the base material are in agreement with the coordinate system given in Figure 6.

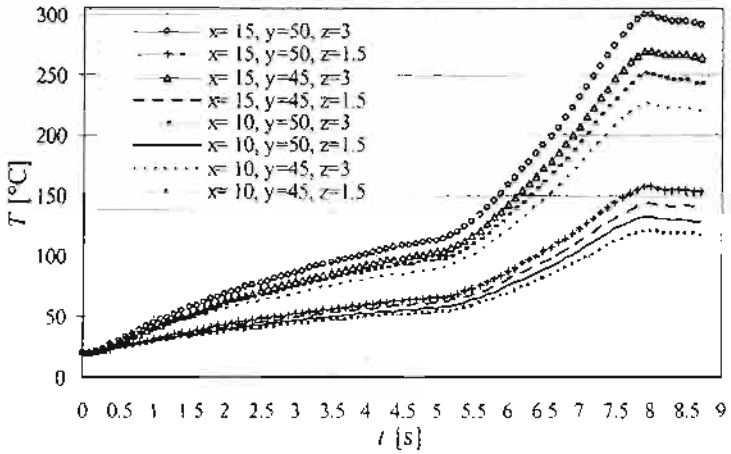

Fig. 9 Analytically estimated temperatures of some specific points on base material during plunging phase

Considering sliding as a dominant mechanism of heat generation, assuming that plastic strain can be disregarded (for the plunging phase), using temperatures given in Fig. 9 and data given in Table 1, it is not difficult to analytically estimate expected values of yield strength σ_{yield} during the plunging phase.

Fig. 10 shows the values of the monitored plunging force $F(t)$, the monitored engaged power on the welding tool $P(t)$ and the analytically estimated generated heat $Q(t)$.

6.3 Discussion of results

When comparing the analytically estimated generated heat and the experimental power (Fig. 10), it is obvious that there is significant similarity between them regarding shape, character and values. The trend of the analytical power is the same as the trend of the experimental power. The highest value of relative error between the analytic and the experimental power is 19.2%. The analytically estimated heat has slightly higher values than the experimental heat almost throughout the complete plunging phase. This can be attributed to the fact that the efficiency factor of the machine and transmission are neglected during the analytical estimation as well as to the mentioned approximations.

7. CONCLUSIONS

Heat generation during FSW is probably the most important product of the intimate contact between the welding tool and the base material - mechanical power delivered to the welding tool is in great amount transformed into heat. However, it is very difficult to explain this important physical process mathematically because it depends on numerous tribological parameters that are mutually entwined and changing. Recognizing the importance of heat generation for FSW, numerous researches and investigations have been conducted with a goal to reveal some of the tribological processes that appear during FSW and to advance the understanding of the FSW process and heat generation. Various mathematical models for the analytical estimation of heat generation have been developed and this paper has summarized most of them, developed some new ideas, and applied them on FSW. The plunging phase is recognized as the phase in which force and power reach their maximum and the complete FSW process has to be modelled according to the requirements of the plunging phase. The welding machine has to be capable of overcoming resistances during the plunging phase

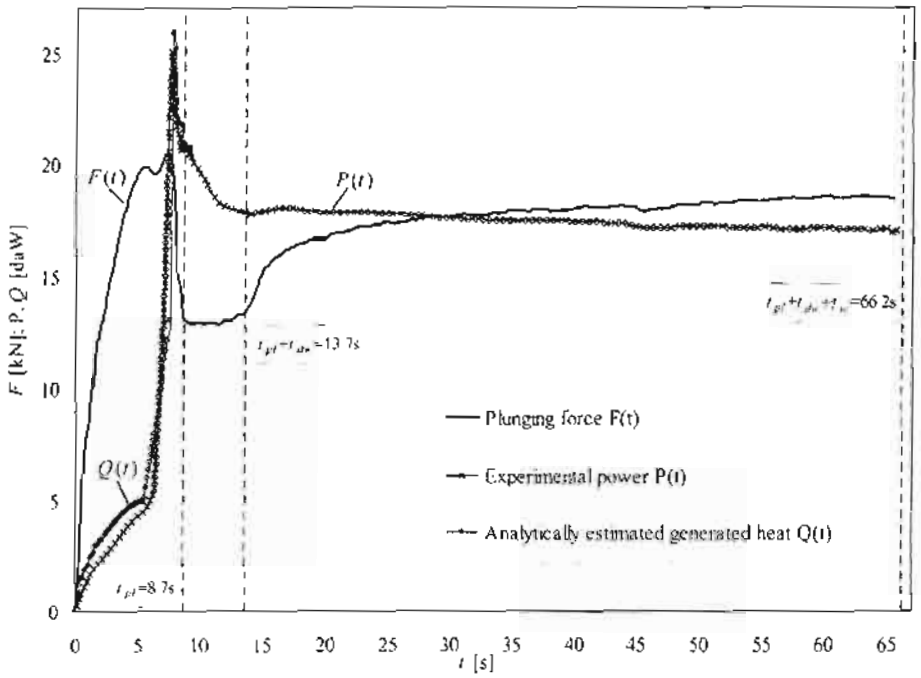

Fig. 10 Experimental plunging force, engaged power [20] and analytically generated heat

Sliding is a dominant mechanism for heat generation during most of the plunging phase. Sliding loses its dominance when the contact pressure between the welding tool and the welding plate reaches a critical value.

The assumption that sliding and sticking equally ($\delta = 0.5$) influence the total amount of generated heat Q (t) is questionable. Some active surfaces are minimally involved in deformation during some period and at some other moment they are completely involved in sliding. Dimensionless slip rate δ should not be considered as a constant value.

The analytically estimated maximal generated heat, together with the maximal plunging force, both achieved during the plunging phase, can be used as design values of the FSW process. The maximal value of the needed plunging force F_{max} (t) during plunging can be estimated as a value when the median contact pressure p_m (t) exceeds the critical contact pressure $k \cdot \sigma_{Yield}$. This value F_{max} (t) is used for the calculation of the generated heat Q, the temperature field of the base material (temperature T) and the maximal value of the generated heat Q_{max}. When the values of the maximal plunging force F_{max} (t) and the maximal engaged power $P = Q_{max}$ are familiar values it is not difficult to select a machine capable of fulfilling requirements of a selected FSW process.

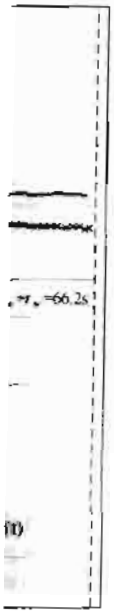

ACKNOWLEDGMENT

Authors would like to thank Professor Miroslav B Durđanović, retired professor of the University of Niš, Faculty of Mechanical Engineering, Niš, Serbia, for providing us with the inspiration for dealing with the problem of heat generation as well as for his unselfish and honest ideas and suggestions that made it possible for us to complete our work on the issues presented in this paper.

The paper presents preliminary results of the research project TR35034 – "An investigation into modern non-conventional technologies: applications in manufacturing companies with the aim of increasing efficiency of use and product quality, of reducing costs and of saving energy and materials". The project is supported by the Ministry of Science and Technological Development of the Republic of Serbia.

REFERENCES

[1] Thomas W M et al. 1991 Friction stir butt welding International Patent Application No PCT/GB92/02203; Thomas W M et al. 1995 Friction stir butt welding GB Patent Application No 9125978.8; Thomas W M et al 1995 Friction stir butt welding UP Patent No 5 460 317.

[2] Santiago, Diego; Urquiza, Santiago; Lombera, Guillermo and Vedia, Luis de. 3D modelling of material flow and temperature in Friction Stir Welding. Soldag. insp. (Impr.) 2009, vol.14, n.3, pp. 248-256.

[3] Gould, J.E.; Feng, Z. Heat flow model for friction stir welding of aluminum alloys, J. Mater. Process. Manu., v.7, 1998.

[4] Rosenthal, D.; Schirmerber, R. Thermal study of arc welding, Welding Journal, v.17, p.208, 1938.

[5] Chen, C. M.; Kovacevic, R. Finite element modeling of friction stir welding - thermal and thermomechanical analysis, Int. J. Mach. Tool. Manu., v.43, p.1319-1326, 2003

[6] Song, M., Kovacevic, R. Thermal modeling of friction stir welding in a moving coordinate system and its validation, Int. J. Mach. Tool. Manu., v.43, p.605-615, 2003.

[7] Ulysse, P. Three-dimensional modeling of the friction stir-welding process, Int. J. Mach. Tool. Manu., v.42, p.1549-1557, 2002.

[8] Colegrove, P.A.; Shercliff, H. R. 3-Dimensional CDF modelling of flow round a threated friction stir welding tool profile, J. Mater. Process. Tech., v.169, p.320-327, 2005

[9] Nandan, R. et al., Numerical modelling of 3D plastic flow and heat transfer during friction stir welding of stainless steel, Science and Technology of Welding and Joining, v.11, p.526-537, 2006.

[10] Nandan, R. et al., Three-dimensional heat and material flow during friction stir welding of mild steel, Acta Materialia, v.55, p.883-895, 2007.

[11] Chao Y J and Qi X 1999 1st Int. Symp. on Friction Stir Welding (Thousand Oaks, CA. USA)

[12] Frigaard Ø, Grong Ø and Midling O T 2001 Metall. Mater. Trans. A 32 1189–200.

[13] Frigaard Ø, Grong Ø, Bjørneklett B and Midling O T 1999 1st Int. Symp. on Friction Stir Welding (Thousand, Oaks, CA).

[14] Russell M J and Shercliff H R 1999 1st Int. Symp. on Friction Stir Welding (Thousand Oaks, California, USA).

[15] Colegrove P 2000 2nd Int. Symp. on Friction Stir Welding (Gothenburg, Sweden).

[16] Shercliff H R and Colgrove P A 2002 Math. Modelling Weld. Phenom. 6 927–74, Reynolds A P, Deng X, Seidel T and Xu S 2000 Proc. Joining of Advanced and Specialty Materials (St Louis, MO, ASM International) pp 172–7.

[17] Xu S, Deng X and Reynolds A P 2001 Sci. Technol. Weld. Joining 6 191–93.

[18] Khandkar M Z H, Khan J A and Reynolds A P 2003 Sci. Technol. Weld. Joining 8 165–74.

[19] Shi Q, Dickerson T and Shercliff H R 2003 4th Int. Symp. on Friction Stir Welding (Park City, UT, USA).

[20] H Schmidt, J Hattel and J Wert: An analytical model for the heat generation in Friction Stir Welding. Modelling Simul. Mater. Sci. Eng. 12 No 1 (January 2004) p. 143-157. PII: S0965-0393(04)69225-4.

[21] Bowden, F.P. and Tabor, D. Friction – An Introduction to Tribology, Anchor Press / Doubleday. Reprinted 1982, Krieger Publishing Co., Malabar 1973.

[22] L.A. Galin: Contact Problems; The legacy of L.A. Galin, Series: Solid Mechanics and Its Applications, Vol. 155, Galin, L. A., Gladwell, G.M. (Ed.), Original Russian edition published by Nauka, Moscow, Russia, 1953, 1980, 2008, XIV, 318 p., Hardcover, ISBN: 978-1-4020-9042-4.

[23] Tabor, D.: A Simple Theory of Static and Dynamic Hardness, Proceedings of the Royal Society of London. Series A, Mathematical and Physical Sciences, Vol. 192, No. 1029 (Feb. 4, 1948), pp. 247-274, Published by: The Royal Society.

[24] Bülent Yavuz, A. Erman Tekkaya: Correlation between Vickers Hardness Number and Yield Stress of Cold-Formed Products, UMTIK-2008, 13th International Conference on Machine Design and Production, September 3-5, 2008, Istanbul, Turkey.

[25] Hedrih (Stevanović) K., Izabrana poglavlja Teorije elastičnosti, Mašinski fakultet Niš. (Some Chapters in Theory of Elasticity, Faculty of Mechanical Engineering Niš), 1976 and 1988.

[26] Stamenković, D, Đurđanović, M: Tribologija presovanih spojeva (Tribology of the Press Fit Joints). Mašinski fakultet Niš, Srbija, 2005, ISBN – 86 – 80587 – 48 – 6.

[27] Đurđanović, M. "Prilog razmatranju primene toplote generisane trenjem", Tehnika - Mašinstvo, vol. 52, no. 6, pp. 1-7, 2003.

[28] Kragelski IV, Dobychin MN, Kombalov VS. Friction and Wear: Calculation Methods. (Translated from Russian by N Standen) Pergamon Press: Oxford, 1982.

[29] H. Schmidt, J. Hattel: Thermal modeling of friction stir welding, *Scripta Materialia*, Volume 58, Issue 5, Pages 332-337, 2008.

[30] Olaf Lahayne, Josef Eberhardsteiner, Roland Reihsner, Tribological Investigations carried out by a Linear Friction Tester, Transactions of Famena, FAMENA issue 2, volume 33, pp. 15 - 22 , Zagreb, Croatia, 2009.

[31] Đurđanović Miroslav, Mijajlović Miroslav, Milčić Dragan, Stamenković Dušan: Heat Generation During Friction Stir Welding Process, Tribology in Industry, no. 1-2, 2009, Serbia, Kragujevac, Faculty of Mechanical Engineering Kragujevac, May, 2009, Journal, vol. 31, pp. 8-14, no. 1-2, ISSN 0354-8996.

[32] EN 573-3:2007, Aluminium and aluminium alloys - Chemical composition and form of wrought products - Part 3: Chemical composition and form of products, EN 485-2:2008-10, Aluminium and aluminium alloys — Sheet, strip and plate — Part 2: Mechanical properties.

[33] The American Society for Metals, Metals Handbook 10th ed., vol 2: Properties and Selection: Non Ferrous Alloys and Special – Purpose Materials, ASM International, 1992.

Submitted: 28.11 2010

Accepted: 04.3.2011

Miroslav Mijajlović, M.Sc ME, IWE
University of Niš, Faculty of Mechanical Engineering, Niš, Serbia
mijajlom@masfak.ni.ac.rs

Prof. dr Dragan Milčić
University of Niš, Faculty of Mechanical Engineering, Niš, Serbia

Prof. dr Dušan Stamenković
University of Niš, Faculty of Mechanical Engineering, Niš, Serbia

Mr. Aleksandar Živković, M Sc ME, EWE
Goša FOM, Smederevska Palanka, Serbia

Dimitra Tzourmakliotou

ISSN 1333-1124

BROADENING OF THE REPERTOIRE OF FORMS FOR SPACE STRUCTURES BY USING FORMEX ALGEBRA

UDC 512.7

Summary

Remarkable progress in computer aided techniques has made possible for architects and engineers to design and realize more and more complicated and innovative structural forms with ease and elegance. The visualization and analysis of any structure, including a space structure, on a computer requires information about various aspects of the structural system. This information could be initially used for graphical visualization of the structure, or may be submitted as input data to an analysis package. Therefore, it is important to have a convenient system for manipulating and changing various aspects of the form to examine different solutions. Formex algebra is one such mathematical system. The concepts of formex algebra are presented in this paper in relation with the Formian, which is in fact the programming language of formex algebra. This paper presents a methodology for generating and manipulating space structure forms using computer aided techniques based on formex algebra

Key words: *formex algebra, Formian, structural forms, retronorms*

1. Introduction

For large and complex structural forms, the sheer volume of information to be handled can make data generation a time consuming and a difficult task. To overcome this problem, suitable systems have been developed by which computer graphics and data generation for any type of structure can be done conveniently. Formex algebra is one such mathematical system. The ideas of formex algebra can be applied to many braches of science and technology; in the present paper, they have been described in relation to a variety of space structure configurations.

Configurations may be described using numerical models. In particular, when digital computers are involved, the internal representation of a configuration is bound in terms of a numerical model. The term "configuration processing" is used to mean "creation and manipulation of numerical models representing configurations". Formex algebra is a mathematical system which is ideally suited for configuration processing. In using the formex approach, a "formex" (plural formices) is used to represent a configuration. The main role of a formex is to provide information regarding the constitution of a configuration. In addition, a formex may be used to provide geometric information about a configuration in terms of coordinates of nodal points. The concepts of formex algebra are discussed in this paper together with the Formian [1]. The Formian is a suitable computing software that can solve problems of computer graphics and data generation in an effective and elegant way [2], [3].

Transactions of FAMENA

UNIVERSITY OF ZAGREB

FACULTY OF MECHANICAL ENGINEERING AND NAVAL ARCHITECTURE

HR – 10 000 ZAGREB, Ivana Lučića 5

☎ 01 61 68 540 / Fax 61 68 187

e-mail: jasna.biondic@fsb.hr

http://famena.fsb.hr/famena.php

Instructions to Authors

1. *Transactions of FAMENA* will publish original scientific papers, preliminary notes, subject reviews and professional papers. In the Appendix the Journal will publish book reviews, conference announcements, obituaries etc
2. The language of the journal is English. Only local news may be printed in Croatian.
3. For the purpose of reviewing, manuscripts should be submitted as hard-copy printout (4-fold) to Editor-in-Chief or Co-Editor. The manuscripts must be typewritten, double-spaced with 3 cm margins on one side of A4 paper. The pages and appendices must be numbered.
4. The title page has to comprise the title, the author(s) and the author's affiliation and full address. Correspondence will be sent to the first-named author, unless otherwise indicated.
5. The abstract must not exceed 150 words in length with 3-5 keywords.
6. Tables and Figures should be placed on separate sheets, with an indication in the text as to their appropriate placement.
7. Follow this order when typing manuscripts: Title page, Abstract, Keywords, Main text, Acknowledgements, Appendix, References and then Captions for figures and tables.
8. Mathematical symbols and formulae should be typed. Particular care should be exercised in identifying all symbols and in avoiding ambiguities.
9. References to published literature should be cited in the text using numbers in square brackets, e. g. [1], and arranged in alphabetical order in a Reference section.
10. Reviewers will be asked to provide comments on the manuscript, which will then be forwarded to the authors. The reviewing time will normally be 6 to 10 weeks.
11. After acceptance, the author(s) will be asked to submit the final version of the manuscript and figures in electronic form in addition to a hard-copy printout.
12. No manuscript or figures will be returned following publication unless a request for return is made when the manuscript is originally submitted.

Transactions of FAMENA

Faculty of Mechanical Engineering and Naval Architecture
University of Zagreb
Ivana Lučića 5, Zagreb, Croatia
http://famena.fsb.hr/famena.php

Transactions of FAMENA has been published as:

Zbornik radova FSB (in Croatian)	Vol. I – XIX	1970. - 1996.
Radovi FSB - Acta (in Croatian)	Vol. XX – XXIII	1997 - 1999.
Transactions of FAMENA – Radovi FSB	Vol. XXIV –	2000. -

Transactions of FAMENA is indexed/abstracted in:

Science Citation Index Expanded
Journal Citation Reports/Science Edition
GEOBASE, Water Resources Abstracts
CSA Engineering Research Database
Scopus

ISSN 1333 – 1124

Prints 250

Address: Faculty of Mechanical Engineering and Naval Architecture, University of Zagreb,
Ivana Lučića 5, HR-10000 Zagreb, Croatia
☎ : ↔ 385 01 61 68 540 or Fax: ↔ 385 01 61 68 187; *e-mail: jasna.bondic@fsb.hr*
Account No.: 2360000-1000000013 or **Swift:** ZABA,HR,2X 2500 3276546
Zagrebačka banka, Savska 66, Zagreb, Croatia „«Transactions of FAMENA»
Broj žiro računa: 2360000-1101346933 s naznakom «za časopis Transactions of FAMENA» (samo za Hrvatsku)
Annual subscription rate (four issues): For Europe: 120 EURO
Obavijest o godišnjoj pretplati (četiri broja): Za Hrvatsku: pretplata 900 kn

The editing of this Journal has been partly supported by the
Ministry of Science, Education and Sports of the Republic of Croatia

ISSN 1333-1124